analytical chemistry

ARTICLE

pubs.acs.org/ac

Investigating the Superhydrophobic Behavior for Underwater Surfaces Using Impedance-Based Methods

Juan C. Tuberquia, Won S. Song, and G. Kane Jennings*

Department of Chemical and Biomolecular Engineering, Vanderbilt University, Nashville, Tennessee 37235, United States

Supporting Information

ABSTRACT: We have investigated the impedance behavior of immersed superhydrophobic (SH) polymethylene surfaces by tailoring the surface tension of the contacting liquid phase to gradually transition the surface from the Cassie to the Wenzel state. Control over the surface tension is accomplished by varying the ethanol content of the aqueous phase. To establish the mechanism of the transition, we imaged the interface of the film and identified three distinct events of this process: a nucleation event at low concentrations of ethanol in which small areas beneath the liquid phase transition into the Wenzel state, a propagation event characterized by the enlargement of the Wenzel domains and the lateral displacement of air, and a final event at higher concentrations of ethanol in which the thin air layer at the interface morphs into isolated pockets of air. Using this visualization of the transition, we characterized the Cassie and the Wenzel states by measuring the impedance at a frequency of 1 kHz for an initially SH film that changes its wetting behavior upon addition of ethanol. Establishment of the Cassie and Wenzel state conditions was based on concepts of electrochemical impedance spectroscopy (EIS) and quantitatively validated using both the Helmholtz theory and the analytical description of the electrochemical system in terms of the circuit model of a metal surface covered by a polymer film. Finally, we apply this strategy to determine the possibility for SH polymethylene (PM) films to reversibly transition between the Cassie and the Wenzel states. Results show that after rinsing and drying at ambient conditions for 24 h, the film recovers the SH state, suggesting the applicability of these SH films in outdoor environments with occasional periodic submersion in water.

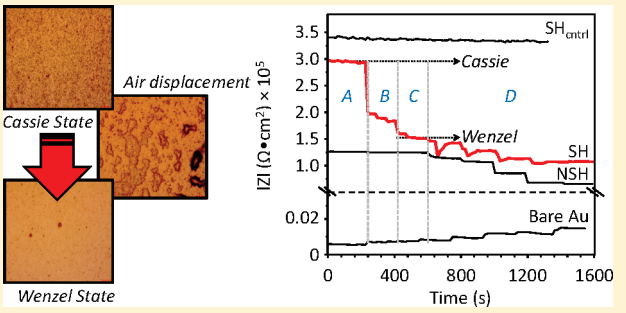

The performance of coatings in applications such as corrosion protection, anti-icing,[1] and self-cleaning,[2] among others, is greatly enhanced if the surface of the coating is superhydrophobic (SH) or in the Cassie state of wettability.[3] In this type of wetting state, the rough topography and the intrinsic hydrophobicity of the surface result in limited contact between the liquid phase and the film such that water interacts only at the top of the microscale features decorating the film. In the opposite case, the Wenzel state, water displaces the air present in the grooves of the film and completely wets the contours of the film. Note that these definitions are accepted and widely used from the perspective of contact angle (CA) measurements. However, in the case of a surface immersed in water, we extrapolate and use these classifications based on their physical description. On the basis of these definitions, the design of SH surfaces should account not only for the basic compositional and geometrical requirements[3] that impart such behavior but also for those factors that favor their stability[4] and enhance their robustness. In the last 10 years important research efforts have been made toward the optimization of the geometrical conditions (shapes, aspect ratios, spacing, roughness conditions),[3] fabrication methods,[5−7] and materials[8,9] that impart superhydrophobicity. However, in terms of their stability, establishment of the conditions that drive the transition from the Cassie to the Wenzel state as well as the mechanism in which this process occurs are precise details that still remain unclear.[4,10]

CA measurement is considered the traditional technique to understand the Cassie−Wenzel transition due to its facile implementation and interpretation.[11−13] However, analysis by CA focuses on the events occurring at the triple contact line[12,14] and is blind to those occurring beneath the body of liquid. To circumvent these limitations, transmission diffraction[15] or a combination of optical microscopy and CA[16] have been used to monitor changes beneath the liquid as the surface transitions from the Cassie to the Wenzel state. However, information provided by these techniques, although qualitatively valuable, does not consider the effect of the vertical position of the liquid/vapor interface, a vital piece of information in determining the activation energy required for the Cassie−Wenzel transition.[4]

To characterize the Cassie to Wenzel transition for SH films in underwater environments, we use electrochemical impedance spectroscopy (EIS). In this technique, the film/liquid interactions are measured in the form of a general resistance against the interaction of ions in solution with the underlying substrate,

Received: March 18, 2011
Accepted: June 22, 2011
Published: June 22, 2011

defined as impedance. With this picture in mind, the fundamental differences between the Cassie and the Wenzel wetting regimes are translated into major differences in impedance. In the case of the Wenzel state, lower impedances are exhibited since the liquid wets the contours of the features[17] decorating the film, resulting in both a lower separation between the liquid and the underlying substrate as well as a greater area of contact available for the diffusion of liquid. However, in the case of the Cassie state, two dependent mechanisms are responsible for the higher impedances. The first mechanism is based on the fact that the liquid is sustained on the top of the microscale features[18] leading to a minimization of the liquid/film interaction.[18,19] This aspect has been widely studied for SH films since it is the basis for the CA measurements. The second mechanism responsible for the higher impedances, and one that cannot be completely addressed only by the use of CA measurements,[4] is related to the actual separation of the liquid from the underlying substrate. To exemplify this aspect, Oner and McCarthy[3] showed that SH surfaces with identical chemical composition and physical parameters, except for the height of the microscale features decorating the surface, exhibit similar solid/liquid interactions such that their CAs are identical. However, in the case of the impedance characterization, the measurement of a general resistance against the flow of current between the solution and the underlying substrate inherently accounts for both the wetting behavior and the height of the microscale features such that the film with the highest microscale features would exhibit the largest impedance. In this context, EIS is a powerful technique because it accounts with great sensitivity the surface−liquid interaction, meaning how water wets the surface as well as the effective separation between the liquid and the surface,[20,21] as demonstrated in our previous work.[5,21]

Recent advances in our group have shown that, in the case of SH polymethylene (PM) films, air entrapment results in a dramatic enhancement of the resistance against ion transfer to greater than 10^{10} $\Omega \cdot cm^2$, which is >1000 times greater than a smooth PM film of similar thickness. Further, the capacitances of SH films are far below what is measured for a smooth PM film of similar average thickness.[21] To explain this dielectric effect we have developed an equivalent-circuit-based model of the SH film that accounts for the entrapped air by a simple correction to Helmholtz theory.[21] Our model shows that the inverse capacitance of SH coatings can be expressed in equation form as

$$\frac{1}{C_{film}} = \frac{d_{effective}}{\varepsilon_0 \varepsilon_{effective}} = \frac{\psi d_{film}}{\varepsilon_0 \varepsilon_{PM}} = \frac{\psi}{C_{PM}} \quad (1)$$

where C_{film} is the capacitance of the PM film per unit area, $\varepsilon_{effective}$ is the effective dielectric constant of the film, ε_{PM} is the dielectric constant for PM (2.3), ε_0 is the permittivity of free space, $d_{effective}$ is the effective thickness of the film, defined as the separation distance between the electrolyte solution and the metal substrate, and d_{film} is the average or measured thickness of the film. ψ, according to our model, is a correction factor ($\psi \geq 1$) that depends on the geometrical parameters of the surface and is applied to describe the effect of superhydrophobicity and the associated air entrapment on the dielectric properties of polymer films. For SH PM films prepared by our methods, $\psi \sim 1.8 \pm 0.3$, which translates into an effective thickness (average distance for water−substrate separation) that is ∼40% higher than a smooth film of identical average thickness and a dielectric constant that is 1.7, ∼25% lower than that of the bulk polymer (2.3), due to the incorporation of air at the aqueous/film interface. Thus, the impedance of the film differs markedly in the Wenzel and Cassie states, thereby offering a powerful tool to identify and characterize both states.

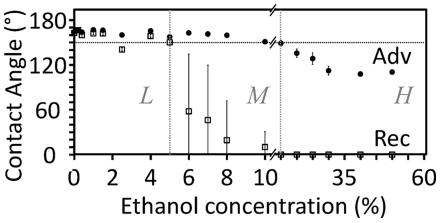

Figure 1. CA measurements as a function of the mass fraction of ethanol. CA behavior exhibits three distinctive regions depending on the ethanol concentration. In region L (0−5%) the film exhibits SH behavior, in region M (5−15%) the film exhibits both high advancing (>150°) and high hysteresis values ($\theta_A - \theta_R < 10°$), and in region H (15−50%) the features decorating the film are completely wet.

In this paper, we use SH PM films grown from surface-initiated polymethylenation[5] to study the transition of immersed films from the Cassie to the more stable Wenzel state. To do this, instead of waiting on the natural kinetics of the system to accomplish such change, we direct the transition by gradually reducing the surface tension of the liquid phase, initially 71.3 mN/m for pure water, through discrete additions of ethanol (γ_{EtOH} = 23 mN/m). To monitor possible changes at the solid/liquid interface upon ethanol addition, we use CAs to establish the implicit wetting behavior of an SH film when the surface is in contact with aqueous solutions of specific ethanol concentrations, optical microscopy to visualize the form in which the Cassie to Wenzel transition occurs, and EIS measurements to monitor reductions in the effective separation between the liquid and the underlying substrate from changes in the impedance of the system.[21] Finally, we applied this strategy to determine the reversible character of SH PM films after loss of the Cassie state due to displacement of the air entrapped at the solid/liquid interface.

RESULTS AND DISCUSSION

Contact Angles. We used advancing and the receding CA measurements as indicators of the interactions that occur between an SH surface and ethanol−water solutions of different surface tensions (γ_{sol}). Figure 1 shows that the CA behavior has three distinctive regions depending on the concentration of ethanol: region L, for small amounts of ethanol (0−5%), in which the film exhibits SH behavior ($\theta_A > 150°$, $\theta_A - \theta_R < 10°$),[2,22] region M, at intermediate concentrations of ethanol (5−15%), in which the film exhibits both high advancing CA (>150°) and high hysteresis values ($\theta_A - \theta_R < 10°$), and region H, for high concentrations of ethanol (15−50%), in which the liquid completely wets the contours of the microscale features decorating the film. For more detailed information regarding the γ_{sol} behavior and the advantages of the water−ethanol system, please refer to the Supporting Information.

Figure 1 shows that the addition of ethanol to water results in substantial changes in the interaction between the liquid phase and the polymer surface. We observe that, in region L, the advancing and receding CAs do not exhibit any measurable changes as γ_{sol} is reduced (57 mN/m < γ_{sol} < 71.3 mN/m), indicating that, as the aqueous drop is placed on the surface, the Cassie regime is maintained. On the other hand, in region H, the

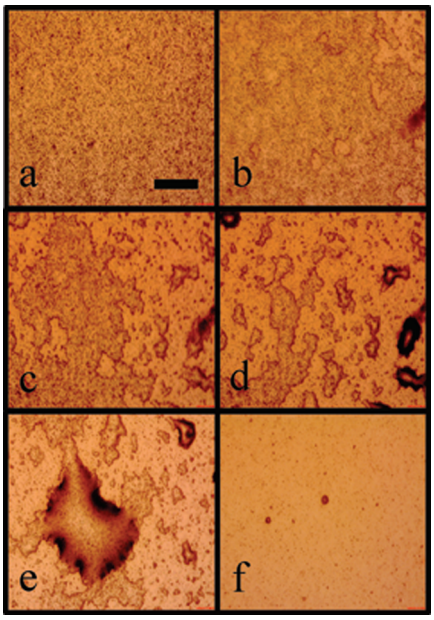

Figure 2. Optical microscopy images of the interface of an SH PM film in contact with water−ethanol solutions of various concentrations: (a) the interface is in the Cassie state when in contact with pure water; (b−d) the interface transitions from a primarily Cassie to a primarily Wenzel state when in contact to a 9% ethanolic solution (the time frames of panels c and d in relation to panel b were 10 and 15 min, respectively); (e) an air pocket that results from the expansion of the Wenzel state along the interface of the film (the film is in contact with a 13% ethanolic solution); (f) the interface at a different location from (e) is in the Wenzel state when in contact with a 13% ethanolic solution. The bar in panel a indicates a length of 100 μm.

reduction in γ_{sol} (44 mN/m < γ_{sol} < 28 mN/m) results in a limiting advancing CA of 110°. This value is close to that exhibited for smooth PM films in contact with water (~103°)[23] and could be interpreted as a reasonable value for the Wenzel state advancing CA since the values for the roughness ratio calculated from the Wenzel equation (1.52) and the polymer/water contact fraction that would render SH behavior from the Cassie equation (<10%) are in agreement with values published in the literature for SH surfaces.[2,22,24] At these conditions, we envision that placement of the drop on the surface results in the instantaneous movement of the liquid phase from the top to the base of the microscale features decorating the surface. Finally, the intermediate region M could be considered as a transition region in which a punctual description of the wetting behavior is not straightforward to define, except that the film is no longer SH for ethanol concentrations greater than 5%. Note that the absence of the SH behavior in this region does not necessarily imply that the entire film transitioned into the Wenzel state. These CA results show that specific additions of ethanol to an aqueous solution allow for the tuning of the wetting behavior of the aqueous solution in contact with an SH surface.

Optical Microscopy. To visualize the Cassie to Wenzel transition, Figure 2 shows the images of an SH interface (162°/162°) immersed in an aqueous solution of various ethanol concentrations. To collect the images, the probe film is completely covered with a 13 mm column of water followed by discrete additions of ethanol to target specific concentrations without agitating the system. Figure 2a shows the interface when pure water sits on the top of the microscale features decorating the surface. In contrast to this behavior, Figure 2f is an image of the interface after the aqueous solution (13% in weight of ethanol) penetrates into the grooves and completely wets the contours of the surface. Using the visualization of these extreme cases, we observe in Figure 2b−d various stages of the transition for this particular spot of the film in which the interface changes from primarily Cassie behavior to primarily Wenzel behavior when in contact with a 9% ethanolic solution. The images of Figure 2, parts c and d, were obtained 10 and 15 min, respectively, after Figure 2b was obtained. Visualization of the interface shows that the transition begins with the nucleation of the Wenzel state at relatively small and randomly located areas of the interface. This event is followed not only by further creation of nucleation sites but also by the lateral expansion of the areas in the Wenzel state as a result of the lateral displacement of air and its subsequent accumulation to form individual air pockets as shown in Figure 2e for a higher ethanol concentration. The localized character of the transition does not allow us to determine the critical amount of ethanol that triggered the transition since the monitored area is much smaller than the area of the film, meaning that the area under observation could remain in the Cassie state by the time that other parts of the film have already transitioned into the Wenzel state. However, visual observation of different areas of the film, as well as impedance results (vide infra), indicate that the amount of ethanol required to initiate the transition is much smaller. Finally, these results suggest that the entire surface would eventually exhibit the Wenzel state if more time is allowed or if ethanol is further added into the system or the solution is agitated. Optical microscopy results show visual confirmation of the Cassie to Wenzel transition and also confirm the ability of our strategy to trigger the transition by varying the ethanol concentration.

Single-Frequency EIS. Control over surface tension and ultimately over CA enable the controlled transition from the SH Cassie state to the non-SH Wenzel state for PM films. This level of control over the wetting transition will help to reveal specific details about the mechanism in which this process occurs and to enhance our understanding about the design conditions that stabilize the Cassie state. In this context, EIS not only depends on the surface−liquid interaction, meaning how the liquid probe wets the surface, but also, it accounts, with great sensitivity, for the effective separation between the liquid and the surface,[20,21] an aspect as important as the spacing and the contact area of the microscale features in determining the activation energy required for the Cassie−Wenzel transition.[4]

To describe the way superhydrophobicity can be addressed by EIS, we note that the values of impedance ($|Z|$) and phase angle (ϕ) reported by this technique describe the magnitude and direction of the complex impedance vector, respectively.[20] This convenient description of the impedance allows for the accounting of the capacitive

$$Z_{Im} = \frac{1}{\omega C} \tag{2}$$

and resistive contributions of the film

$$Z_{Re} = R \tag{3}$$

by using them as the imaginary and real components, respectively, of the impedance vector.

$$\bar{\mathbf{Z}} = Z_{Re} - jZ_{Im} \tag{4}$$

The phase angle can be understood as a relative indicator of both contributions, being zero for a purely resistive film in which

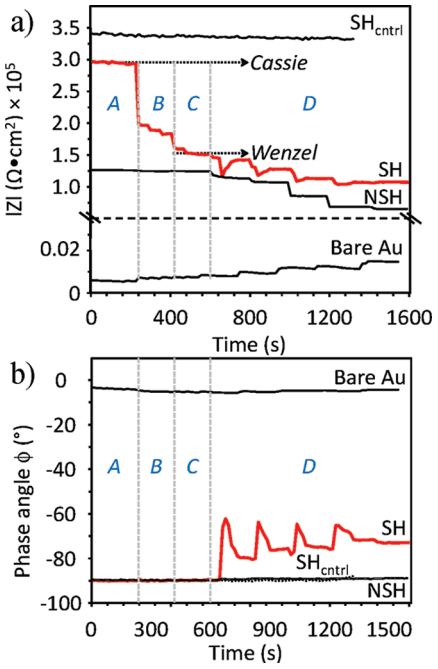

Figure 3. Impedance at 1 kHz (a) and phase angle (b) of an SH film (SH) upon additions of ethanol. For proper understanding of the transition process, we also determine the impedance behavior for an SH PM film exposed to pure water (SH_{cntrl}) and both a bare gold substrate (bare Au) and a smooth PM film (NSH) that followed ethanol additions. Concentrations of the liquid phase targeted a $LiClO_4$ concentration of 0.05 M and specific ethanol concentrations in mass (%) of A (0.6, 3, 8×10^{-3}), B (0.02, 0.16, 0.5), C (0.9, 1.4, 2), and D (4, 9, 13, 17, 21). Ethanol additions were performed every 60 s for regions A, B, and C, whereas in region D they were performed every 200 s.

the liquid and ions are transferring through, −90° for a purely capacitive film that acts as a dielectric to completely separate the liquid from the substrate, and any value in between for a combination of both states. At the SH state, the film provides the largest separation between the aqueous phase and the substrate, resulting in large impedances with a completely capacitive ($\phi = -90°$) behavior. As the SH state begins to break down and transition into the Wenzel state, liquid and ion penetration into the grooves of the film reduces the capacitive impedance due to both air removal and the lower separation between the solution and the substrate. Finally, subsequent penetration of the solution into the film itself leads to a more resistive response and an increase in the phase angle as compared to the completely capacitive state.

To identify the impedance characteristics for both the Cassie and the Wenzel states, we monitor over time the impedance and the phase angle behavior (Figure 3, parts a and b, respectively) for an initially SH PM film (165°/164°) at a single frequency of 1 kHz as discrete amounts of ethanol are added to the system (SH). The single frequency of 1 kHz was selected because, according to complete impedance spectra (see the Supporting Information), the impedance at this frequency has a primarily capacitive behavior ($\phi \sim 90°$), thus allowing interpretation of the data using Helmholtz theory. In addition, single-frequency EIS allows monitoring the impedance at a single frequency over a greater spectrum of concentrations, taking advantage of its in situ character and shorter acquisition time as compared to EIS to rapidly detect the onset of impedance change once the solution begins to displace the air interlayer. To break the SH behavior, we continually increased the ethanol concentration from 0% to 21% in mass according to the specific targets that we have conveniently categorized in regions A (0.6, 3, 8×10^{-3} %), B (0.02, 0.16, 0.5%), C (0.9, 1.4, 2%), and D (4, 9, 13, 17, 21%) while maintaining a constant $LiClO_4$ concentration (0.05 M). To collect the impedance measurements, the probe area (1 cm^2) was completely covered with a 16 ± 1 mm column of $LiClO_4$(aq) and ethanol followed by agitation of the system in the specific case of region D to evacuate any large air pockets that may form at the interface of the film. In regions A, B, and C, ethanol additions were performed every 60 s, whereas in region D, they were performed every 200 s.

For proper understanding of the transition process, we also determined the impedance behavior at 1 kHz for three different controls. As a first control, we exposed an SH PM film to a water and $LiClO_4$ solution (SH_{cntrl}) without ethanol and observed that its impedance behavior remains constant in the time window of the experiment, yielding a purely capacitive contribution ($\phi \sim 90°$). To determine the effect that ethanol additions have on the resistivity of the solution, we analyzed the impedance behavior of a bare gold substrate (bare Au) exposed to the same conditions as that of the SH surface. Upon addition of ethanol, changes in the transport properties of the solution affect the resistance of the solution as indicated by the low phase angle ($\phi < 5°$) in Figure 3. Finally, a smooth non-SH PM film (NSH) that was exposed to additions of ethanol as well serves as a reference to the SH surface. The behavior of the NSH film provides a scenario in which the impedance exclusively depends on the ethanol−PM interactions without any interference from the topography of the film, thus enabling determination of potential swelling of the film. Although topographic characterization of the SH and non-SH PM films was addressed in our previous work,[21] we include SEM here images in the Supporting Information (Figure S3) showing the topographic characteristics of both surfaces. Experimental results show that the impedance of the NSH film remains constant up to ethanol concentrations of 4% and exhibits discrete reductions in its magnitude as the ethanol content increases while maintaining a primarily capacitive behavior ($\phi \sim -90°$) over the time window of the experiment. For the case of the SH film (denoted SH), the impedance decreases in a stepwise manner over the time window of the experiment. However, in contrast to the NSH film, the phase angle of SH film exhibits a primarily capacitive component for ethanol concentrations up to 4% that progressively increases its resistive contribution up to a final value of $\sim -70°$.

Figure 3 establishes proper identification of the Cassie and the Wenzel states after determining the importance of three different aspects: swelling of the PM film, changes in the resistivity of the liquid phase after additions of ethanol, and variations in the impedance of the SH film as air is displaced from the liquid/solid interface. As the ethanol content increases, the ability of the aqueous solution to transport ions reduces,[25] thus resulting in higher impedances as illustrated by the behavior of the bare Au substrate. However, as evidenced in Figure 3a, the magnitude of the impedance for the bare Au substrate does not provide significant contribution to the impedance of the SH film. In terms of swelling, Figure 3b shows that the impedance for the NSH film exhibits primarily capacitive behavior, meaning that the PM film provides a complete separation between the liquid phase and the metal substrate. However, for ethanol concentrations greater than 4%, the impedance of the film does exhibit a reduction in its magnitude, which we attribute to swelling near the solid/

liquid interface to provide a reduced distance of separation between the solution and the electrode. We emphasize that appreciable swelling that would result in ion transfer through the film is not occurring since the phase angle remains near $\sim -90°$. For the case of ethanol concentrations equal or lower than 4%, the impedance of the NSH film remains constant to indicate that no appreciable PM−ethanol interactions are present.

To identify the impedance behavior of the Cassie and the Wenzel states for an SH film, we first qualitatively assess the behavior of the SH film and identify each state according to its characteristics. In region A, since $\phi \sim -90°$ and the impedance modulus exhibits the highest impedance magnitude over the time window, in agreement with the behavior of the SH_{cntrl} control, the film is in the Cassie state. For concentrations of ethanol greater than 0.02%, the impedance of the SH film undergoes a stepwise reduction in impedance as the ethanol concentration increases, suggesting that air is being displaced from the solid/liquid interface. To identify the Wenzel state, we emphasize that, besides its lower impedance compared to that of the Cassie state, the film should also offer a complete separation between the liquid phase and the substrate ($\phi \sim -90°$). According to these characteristics, we observe that regions B and C fulfill these requirements. However, since region C exhibits the lowest impedance, indicative of the smallest liquid−substrate separation, we assign the complete Wenzel state to this region. For the case of region B, the intermediate impedances of the SH film suggest that both the Cassie and the Wenzel states are present beneath the liquid phase, which is similar to the mixed Cassie−Wenzel regime shown in the images of Figure 2b−d. Finally, region D shows that further additions of ethanol slightly reduce the impedance of the film until ultimately remaining constant at concentrations of 17−21%. Impedance results in this region show the appearance of a resistive component ($0° < \phi < 90°$), inconsistent with either the Cassie or the Wenzel impedance behavior, that indicates the penetration of ions into the film due to the porous structure of the SH film[21] (Supporting Information Figure S3a). The absence of a resistive component in the behavior of the NSH film is the product of the compact and nonporous structure of this film[21] (Supporting Information Figure S3b) that completely isolates the substrate from the aqueous media.

To quantitatively validate the Cassie and the Wenzel state assignments of the impedance curve for the SH surface, we compared the $1/C_{Helmholtz}$ predicted by the Helmholtz theory (eq 1) with the $1/C_{Measured}$ that yields the impedances exhibited for both states at 1 kHz according to Figure 3a. For the case of the Helmholtz theory, we calculate the inverse of capacitance ($1/C_{Helmholtz}$) with eq 1 using an average thickness of $d_{film} = 2180 \pm 180$ nm, the dielectric constant (2.3) of PM, and the correction factor, ψ, to account for either the presence (1.8) or the absence (1) of air at the interface (Table 1). To estimate the $1/C_{Measured}$ that results in the Cassie and the Wenzel impedances shown in Figure 3a, we use the analytical description of the electrochemical system in terms of the circuit model of a metal surface covered by a polymer film[21] and equate the expressions for the components of the impedance vector[20] to the average impedances for both states (see the Supporting Information). Experimental results of $1/C$ in Table 1 show that the experimental estimations, $1/C_{Measured}$, agree with the theoretical predictions, $1/C_{Helmholtz}$, thus indicating that the quantitative as well as qualitative descriptions enable valid assignments of both states.

To translate these differences in capacitance into different average heights between the aqueous phase and the metal surface when the film transitions from the Cassie to the Wenzel state, we use the mathematical description of ψ and the Cassie equation to estimate the effective thickness and the effective dielectric constant of the SH film.[21] These calculations indicate that at, the SH state, the effective dielectric constant (1.7) is 26% lower than that of PM, and the effective thickness of the film is 43% higher than the average thickness of the film. The difference in thickness between the Cassie and Wenzel states is ∼950 nm, which is consistent with the microscale nature of the features decorating the film.[5] Finally, to determine the fraction of the interface that undergoes the Cassie to Wenzel transition at a given concentration, we investigate the impedance behavior of the SH surface at region B. For these calculations we assume that the film behaves as a circuit composed of two capacitances in parallel, one for film areas in the Cassie state and the other for areas in the Wenzel state:

$$C_{film} = C_C\varphi_C + C_W\varphi_W \quad (5)$$

where C_i and φ_i are the capacitance per unit area and the area fraction beneath the liquid phase for the component i, respectively, where i refers to the Cassie or Wenzel state. Using eq 5 along with the capacitances of Table 1, we determine that these intermediate capacitances correspond to area fractions in the Wenzel state ranging from 50% to 65% before the ultimate transition into a complete Wenzel state. Thus, the rapid nucleation event that leads to the transition occurs at around half of the interfacial area and is responsible for 70% of the total reduction in impedance, followed by stepwise propagation events until complete transition.

The critical concentrations of ethanol that break the SH behavior are significantly different for CA (5%) versus impedance measurements (0.02−2%). We attribute these differences in the required ethanol concentration to the nature and characteristics of each technique. In the case of the CA measurements, we determine the characteristic behavior of the triple contact line that results from contacting an SH film with a droplet of a specific ethanol concentration. In other words, we focus on the behavior of an aqueous interface when primarily surrounded by air. However, in the case of EIS, we monitor the behavior of the liquid/film interface of an SH film in underwater conditions upon progressive changes in the nature of the liquid phase and in situ displacement of air. More specifically, we focus on the behavior of the micrometer-thick air layer that is entrapped between the polymer and the aqueous solution. Using the description of each technique, we observe that both the air interlayer in EIS and the aqueous droplet in the Cassie state tend to minimize the unfavorable interactions with the environment surrounding them by transitioning to a more stable configuration. In the case of EIS, the air interlayer transitions into submillimeter air pockets randomly distributed along the

Table 1. Electrochemical Parameters of the Cassie and the Wenzel States Calculated for an SH Film

wetting state	ψ	$1/C_{Helmholtz}$ (cm^2/nF)[a]	$\lvert Z\rvert_{av}$ at 1 kHz[b]	$1/C_{Measured}$ (cm^2/nF)[c]
Wenzel	1	1.07	2.95×10^5	0.96
Cassie	1.8 ± 0.3	1.94	1.53×10^5	1.86

[a] The inverse capacitance calculated from the Helmholtz theory (eq 1). [b] The average impedance of each state according to Z_{SH} in Figure 3. [c] The inverse capacitance calculated.

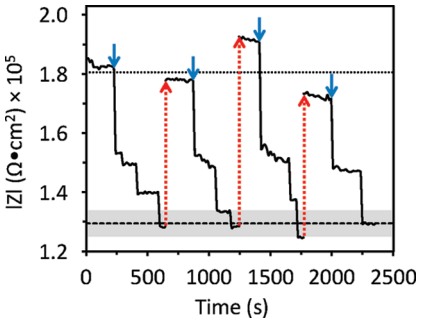

Figure 4. Reversible impedance behavior at 1 kHz exhibited by an SH film 1650 ± 60 nm thick. In the Cassie state, the film is in contact with 0.05 M $LiClO_4$(aq), that upon, addition of ethanol in the same conditions as in Figure 3 up to a final concentration of 4%, transitions into the Wenzel state. To reversibly recover the Cassie state, the film was dried with a stream of nitrogen for 1 min followed by drying at ambient conditions for 24 h.

interface. For CA measurements, the droplet alters its shape as its base makes full contact with the film. The reductions in liquid/air interfacial area for these configurations indicate that the driving force toward the transition of the interface is much higher for SH films in immersed conditions compared to that of CA conditions, corresponding to the observation that smaller amounts of ethanol are required to favor the transition as shown in our experimental results. The higher susceptibility of SH films to transition into the Wenzel state in underwater conditions, as well as the remarkable sensitivity of EIS to detect changes in the separation between the liquid and the underlying substrate, makes impedance a powerful technique to assess the SH properties of films for use in underwater conditions.

Reversibility Test. We have applied the above strategy to assess the ability of SH PM films to reversibly transition back into the Cassie state after reaching the Wenzel state. To perform the reversibility test, we use single-frequency EIS to measure the impedance at 1 kHz of an initially SH film (1650 ± 60 nm) in contact with 0.1 M $LiClO_4$(aq) that transitioned into the Wenzel state after adding ethanol in the same conditions as in Figure 3 to a final concentration of 4%. As a first reconditioning strategy, we reduced the ethanol concentration back below 0.02% after the film transitioned into the Wenzel state. However, the impedance (not shown) exhibited no increase, indicating that the in situ recovery of the Cassie state was not possible. In a second strategy, the films were reconditioned by first rinsing them with water and ethanol and then drying the surface with a stream of nitrogen for 1 min followed by drying at ambient conditions for 24 h. Figure 4 shows the impedance of an SH PM film that reversibly varies its wetting behavior using a combination of additions of ethanol and drying for a total of three reconditioning procedures. Impedance results indicate the ability of the SH film to recover the Cassie state upon drying the liquid phase that transitioned into the grooves of the film. Figure 4 also shows that, upon initiation of the transition, the propagation expands over large areas of the film in a stepwise manner until the entire film exhibits the Wenzel state. Each transition exhibits a different transient profile, suggesting subtle changes in the interface of the film during each reconditioning cycle. Nonetheless, the ability of the film to return to its pristine Cassie state by simply drying the surface in a thorough manner illustrates that these SH surfaces can be regenerated. This characteristic suggests that amphibious coatings such as those exposed to outdoor environments with random periods of moisture could remain in the metastable SH state indefinitely with proper engineering of the coating topography and composition.

CONCLUSION

Control over the Cassie to Wenzel transition by reducing surface tension allows the identification of both states for immersed SH coatings using impedance measurements. Imaging of the interface at different stages of the transition enables the identification of three consecutive events in the process: (1) the nucleation of randomly distributed areas under the Wenzel state, (2) lateral propagation of the Wenzel domains, and (3) the collection of air to form air pockets that would subsequently separate from the surface. The characteristics of the Cassie and the Wenzel states were established using the ideal impedance characteristics of each state and quantified based on the predictions of the Helmholtz theory and the electrochemical description of the polymer film to determine the average height of the air interlayer. Rationalization of the impedance behavior shows that the transition from the Cassie state results from the rapid nucleation of the Wenzel state over half of the solid/liquid interface as evidenced by the 70% impedance reduction of the system, followed by rapid stepwise propagation events until complete transition. Finally, we applied impedance characterization to establish that SH PM films recover their Cassie state after previous transition into the Wenzel state and thoroughly drying the liquid present in the grooves of the film. Experimental results demonstrate the ability of impedance methods to appropriately characterize immersed aqueous SH interfaces and distinguish important wetting states that govern the applications of these surfaces.

ASSOCIATED CONTENT

Supporting Information. Experimental details, along with topographical characterization of the surface using SEM and quantitative validation of the Cassie and the Wenzel states using the electrochemical circuit describing the film. This material is available free of charge via the Internet at http://pubs.acs.org.

AUTHOR INFORMATION

Corresponding Author
*E-mail: kane.g.jennings@vanderbilt.edu.

ACKNOWLEDGMENT

We gratefully acknowledge the financial support of our work to the National Science Foundation (CBET 0731168).

REFERENCES

(1) Cao, L.; Jones, A. K.; Sikka, V. K.; Wu, J.; Gao, D. *Langmuir* **2009**, *25*, 12444–12448.
(2) Callies, M.; Quere, D. *Soft Matter* **2005**, *1*, 55–61.
(3) Oner, D.; McCarthy, T. J. *Langmuir* **2000**, *16*, 7777–7782.
(4) Noscinovsky, M.; Bhushan, B. *Langmuir* **2008**, *24*, 1525–1533.
(5) Tuberquia, J. C.; Nizamidin, N.; Harl, R. R.; Albert, J.; Hunter, J.; Rogers, B. R.; Jennings, G. K. *J. Am. Chem. Soc.* **2010**, *132*, 5725–5734.
(6) Roach, P.; Shirtcliffe, N. J.; Newton, M. I. *Soft Matter* **2008**, *4*, 224–240.
(7) Lee, Y. W.; Park, S. H.; Kim, K. B.; Lee, J. K. *Adv. Mater.* **2007**, *19*, 2330–2335.

(8) Qian, T. C.; Li, Y. F.; Wu, Y. Z.; Zheng, B.; Ma, H. W. *Macromolecules* **2008**, *41*, 6641–6645.
(9) Chen, W.; Fadeev, A. Y.; Hsieh, M. C.; Oner, D.; Youngblood, J.; McCarthy, T. J. *Langmuir* **1999**, *15*, 3395–3399.
(10) Patankar, N. A. *Langmuir* **2004**, *20*, 7097–7102.
(11) Ferrari, M.; Ravera, F.; Rao, S.; Liggieri, L. *Appl. Phys. Lett.* **2006**, 89.
(12) Boinovich, L.; Emelyanenko, A. M.; Pashinin, A. S. *ACS Appl. Mater. Interfaces* **2010**, *2*, 1754–1758.
(13) Lapierre, F.; Thomy, V.; Coffinier, Y.; Blossey, R.; Boukherroub, R. *Langmuir* **2009**, *25*, 6551–6558.
(14) Gao, L.; McCarthy, T. J. *Langmuir* **2007**, *23*, 3762–3765.
(15) Lei, L.; Li, H.; Shi, J.; Chen, Y. *Langmuir*, *26*, 3666-3669.
(16) Colorado, R.; Lee, T. R. *Langmuir* **2003**, *19*, 3288–3296.
(17) Wenzel, R. N. *Ind. Eng. Chem.* **1936**, *28*, 988–994.
(18) Patankar, N. A. *Langmuir* **2010**, *26*, 8941–8945.
(19) Su, Y. W.; Ji, B. H.; Zhang, K.; Gao, H. J.; Huang, Y. G.; Hwang, K. *Langmuir* **2010**, *26*, 4984–4989.
(20) Bard, A.; Faulkner, L. *Electrochemical Methods*, 2nd ed.; John Wiley and Sons: New York, 2001.
(21) Tuberquia, J. C.; Nizamidin, N.; Jennings, G. K. *Langmuir* **2010**, *26*, 14039–14046.
(22) Dorrer, C.; Ruhe, J. *Soft Matter* **2009**, *5*, 51–61.
(23) Seshadri, K.; Atre, S. V.; Tao, Y. T.; Lee, M. T.; Allara, D. L. *J. Am. Chem. Soc.* **1997**, *119*, 4698–4711.
(24) Bico, J.; Marzolin, C.; Quere, D. *Europhys. Lett.* **1999**, *47*, 220–226.
(25) Kay, R. L.; Broadwater, T. L. *J. Solution Chem.* **1976**, *5*, 57–76.